

Low Temperature Heat Capacity and Thermodynamic Functions of $Zr_{0.55}Al_{0.10}Ni_{0.05}Cu_{0.30}$

Atsuko Uchida,[†] Yosuke Moriya,[‡] Hitoshi Kawaji,[†] Tooru Atake,^{*,†} Mikio Fukuhara,[§] Hisamichi Kimura,[§] and Akihisa Inoue[§]

Materials and Structures Laboratory, Tokyo Institute of Technology, 4259 Nagatsuta-cho, Midori-ku, Yokohama, 226-8503 Japan, Department of Chemical System Engineering, Graduate School of Engineering, The University of Tokyo, 7-3-1 Hongo, Bunkyo-ku, Tokyo, 113-8656 Japan, and Institute for Materials Research, Tohoku University, 2-1-1 Katahira, Aoba-ku, Sendai, 980-8577 Japan

The heat capacity of $Zr_{0.55}Al_{0.10}Ni_{0.05}Cu_{0.30}$ alloy was measured for as-prepared glassy, annealed, and crystallized ribbon samples by adiabatic calorimetry from (13 to 300) K. The smoothed values of molar heat capacity were calculated from the data on the basis of a least-squares method. The standard enthalpy, entropy, and Gibbs energy were calculated from the smoothed heat capacity values, and the numerical values of the as-prepared glassy and crystallized samples were tabulated at selected temperatures from (15 to 300) K. The heat capacity, enthalpy, and entropy of the as-prepared glassy ribbon sample at 298.15 K are $25.07 \text{ J}\cdot\text{K}^{-1}\cdot\text{mol}^{-1}$, $5.261 \text{ kJ}\cdot\text{mol}^{-1}$, and $36.80 \text{ J}\cdot\text{K}^{-1}\cdot\text{mol}^{-1}$, respectively, assuming $H(0) = 0$ and $S(0) = 0$ at 0 K. The corresponding values of the crystallized (heated at 877 K for 30 min in a vacuum) ribbon sample are $24.59 \text{ J}\cdot\text{K}^{-1}\cdot\text{mol}^{-1}$, $5.190 \text{ kJ}\cdot\text{mol}^{-1}$, and $36.07 \text{ J}\cdot\text{K}^{-1}\cdot\text{mol}^{-1}$, and the Gibbs energy of the crystallized sample is $-5.565 \text{ kJ}\cdot\text{mol}^{-1}$. The heat capacity of the glassy samples annealed at 508 K and at 641 K in a vacuum is also reported and compared with those of the as-prepared glassy and crystallized samples.

Introduction

Glassy alloys are important functional materials due to their excellent properties such as high strength, and high corrosion resistance, etc., and recently increasing attention has been paid to a variety of applications of superior glassy alloys. The alloys have some local structures, which lead to a wide temperature region of the supercooled liquid state. Such a wide temperature region of the supercooled liquid state is of great advantage in preparing a number of engineering products.

The alloy of Zr–Al–Ni–Cu has a wide temperature region of the supercooled liquid state of about 90 K, and the glassy state can be easily realized in a large bulk size without crystallization.^{1–3} This useful property should be extensively applied in various engineering fields. However, the glassy alloy is in a nonequilibrium state, and the structural, physical, chemical, and mechanical properties are easily changed by some treatments, such as pressurizing and heating, etc. Some studies have been made that especially focus attention on the stability in such thermal annealing.^{4–8} The density of the alloy increases by annealing the as-prepared glassy material at high temperatures and by the following crystallization.^{6,8} This implies that annealing leads to formation of a highly dense random packed structure in the glassy alloy. Such a structural relaxation was also indicated by ultrasonic and hardness measurements.⁶ A thermal relaxation phenomenon was observed in the rapidly cooled glassy ribbon samples by differential scanning calorimetry (DSC),^{5,8,9} as an exothermic anomaly extending from about

400 K up to the glass transition temperature. Such a structural relaxation causes some serious change in the characteristic properties of the glassy alloys and leads to degradation of the materials.¹⁰ Therefore, a fundamental investigation of the annealing effect on the heat capacity is highly required. We have reported preliminary measurements of the heat capacity of glassy and crystallized samples of $Zr_{0.55}Al_{0.10}Ni_{0.05}Cu_{0.30}$ (abbreviated as ZANC) from (2 to 870) K, by DSC and a relaxation method.^{9,11,12} In the present study, we have extended the measurements to the annealing effect on the heat capacity and made precise heat capacity measurements by adiabatic calorimetry for the as-prepared glassy, annealed, and crystallized ribbon samples of ZANC, and determined the values of some standard thermodynamic functions.

Experimental Section

An ingot of ZANC was synthesized from a mixture of Zr, Al, Ni (99.99 % purity), and Cu (99.999 % purity) by arc-melting in an argon atmosphere.¹³ A glassy ribbon sample with a width of 1 mm and a thickness of 20 μm was prepared by a single roller-type rapid quenching method from the melt, in which the sample was vitrified at a cooling rate of about $-10^4 \text{ K}\cdot\text{s}^{-1}$. On the other hand, the glassy rod sample of about 2 mm diameter was prepared at a slower cooling rate of about $-10^2 \text{ K}\cdot\text{s}^{-1}$, and the thermal properties were studied previously.⁹

In the previous scanning DSC measurements of the glassy ribbon and rod samples of ZANC,⁹ we observed a large exothermic curve extending in a wide temperature region from about 400 K to the glass transition temperature around 680 K for the ribbon sample, while no such anomaly was observed in the rod sample up to the glass transition. These results should

* Corresponding author. Tel: (+81)-45-924-5343. Fax: (+81)-45-924-5339. E-mail: ataketooru@mssl.titech.ac.jp.

[†] Tokyo Institute of Technology.

[‡] The University of Tokyo.

[§] Tohoku University.

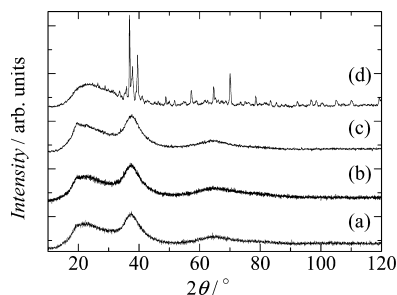


Figure 1. X-ray diffraction patterns of the ribbon samples of $\text{Zr}_{0.55}\text{Al}_{0.10}\text{Ni}_{0.05}\text{Cu}_{0.30}$: (a) as-prepared glassy; (b) annealed at 508 K in a vacuum; (c) annealed at 641 K in a vacuum; (d) crystallized at 877 K in a vacuum.

be attributed to the difference in the randomness frozen in the two glassy states: highly random structure in the ribbon sample, compared to that in the rod sample. Therefore, in the present study on the glassy ribbon sample of ZANC, we have carried out preliminary DSC measurements,¹⁴ to see the effect of thermal treatment that is the annealing effect, before the adiabatic calorimetry. From the DSC experiments, it has been found that the exothermic curve is observed irreversibly depending on the heated temperature.

According to the results of the preliminary DSC, the heat capacity measurements were made using a homemade adiabatic calorimeter as follows. At first, the as-prepared ribbon sample was cut into about a 3 mm length (named as sample a), and then the 8.6067 g (0.114 96 mol) of sample was loaded into the calorimeter vessel (gold-plated copper), which was evacuated and sealed after adding a small amount of helium (5 kPa at room temperature) for the purpose of thermal uniformity within the calorimeter vessel. The contribution of the sample to the total heat capacity including that of the calorimeter vessel was about 20 % to 30 % between 13 K and 300 K.

After the first series of heat capacity measurements of the as-prepared glass ribbon sample, the sample was taken out from the calorimeter vessel and put into a Pyrex glass tube. The tube was evacuated using a rotary pump with a liquid nitrogen trap and then sealed in a vacuum. The sample sealed in a glass tube was annealed in an electric furnace at 508 K for 10 min (named as sample b). Sample b showed no exothermic curve in the DSC measurement below 508 K, but it showed an exothermic curve at higher temperatures up to the glass transition temperature similar to that of the as-prepared sample. The second series of measurements was made for sample b of 6.8980 g (0.092 133 mol). After the second series of measurements, the same sample was annealed by the same method at 641 K for 10 min (named as sample c), and the third series of measurements was made for sample c of 6.5270 g (0.087 178 mol). The DSC run for sample c showed no exothermic curve up to 641 K, and at higher temperatures the DSC curve was very similar to that of the first run of the as-prepared sample. After the third series of measurements, finally the sample was crystallized at 877 K in a vacuum for 30 min (named as sample d), and then the heat capacity was measured on sample d of 5.6705 g (0.075 738 mol). The structural change by these annealing treatments was confirmed by X-ray diffraction as given in Figure 1. Although the curve of (d) shows a rather broad peak around 25 °, it is caused by the fact that the background due to the substrate is not subtracted. The completeness of the crystallization of sample d was confirmed by DSC measurements, which showed no signal due to relaxation/crystallization. Our previous studies^{9,11} also showed the complete crystallization by annealing at 877 K.

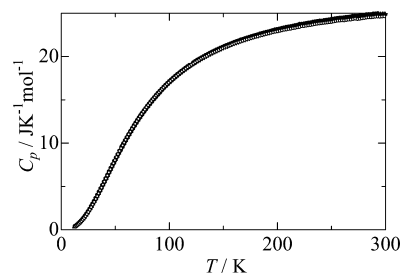


Figure 2. Measured molar heat capacity of the ribbon samples of $\text{Zr}_{0.55}\text{Al}_{0.10}\text{Ni}_{0.05}\text{Cu}_{0.30}$: ●, as-prepared glassy; ▲, annealed at 508 K in a vacuum; ▼, annealed at 641 K in a vacuum; ○, crystallized at 877 K in a vacuum.

The details of the apparatus, the operation, and the performance of the homemade adiabatic calorimeter have been described elsewhere.^{15,16} The temperature was measured with a platinum resistance thermometer (Tinsley, 5187 L) calibrated at NPL on the basis of the international temperature scale (ITS-90). The adiabatic control system gave the temperature stability of the calorimeter vessel within $10^{-5} \text{ K} \cdot \text{min}^{-1}$. The heat capacity of the sample was obtained by subtracting that of the calorimeter vessel from the total heat capacity including the calorimeter vessel. The performance of the calorimeter was confirmed by measuring the standard reference material SRM 720 (synthetic sapphire) provided by NIST, which gave an accuracy of 0.1 % for the measurements of the heat capacity at 100 K.

Results and Discussion

The measured molar heat capacity of the ribbon samples of ZANC is shown in Figure 2, where the data of the as-prepared glassy (sample a), annealed in a vacuum at 508 K (sample b), annealed in a vacuum at 641 K (sample c), and crystallized in a vacuum at 877 K (sample d) samples are plotted. The numerical values of the as-prepared glassy (sample a) and of the crystallized (sample d) samples are tabulated in Tables 1 and 2, respectively. The temperature increment of each measurement was 1 K to 2 K. After each heat input, thermal equilibrium of the whole calorimeter vessel was attained in a few minutes below 20 K and in about 10 min above 100 K. All of the samples have very similar values of heat capacity, and the heat capacity becomes about $25 \text{ J} \cdot \text{K}^{-1} \cdot \text{mol}^{-1}$ at room temperature, which is the classical limiting value of the Dulong and Petit Law. At room temperature, the heat capacity is still increasing, which should be caused by the effects of the thermal expansion ($C_p - C_v$ correction) and the electronic contribution. The smoothed heat capacity curve was obtained from the measured data by a method of least-squares fitting; the heat capacity data were divided into nine temperature regions, and each region was fitted by a polynomial expression up to the seventh power. The heat capacity below 13 K was estimated by a graphical smooth extrapolation down to 0 K. The thermodynamic functions of the as-prepared glassy (sample a) and of crystallized (sample d) samples calculated from the smoothed heat capacity values at rounded temperatures are given in Tables 3 and 4, respectively.

The difference of the molar heat capacity of the glassy samples (samples a, b, and c) from that of the crystallized sample (sample d) is obtained as $\Delta C_p = C_{p(a,b,c)} - C_{p(d)}$, which is shown in Figure 3. The heat capacity of the as-prepared glassy sample (sample a) is the largest in the whole temperature range, and the heat capacity of the glassy samples decreases as the annealing temperature increases. Thus the value of the heat capacity of sample c is the smallest among the three glassy

Table 1. Measured Molar Heat Capacity of the As-Prepared Glassy Ribbon Sample of $Zr_{0.55}Al_{0.10}Ni_{0.05}Cu_{0.30}$

T	C_p	T	C_p	T	C_p
K	$J \cdot K^{-1} \cdot mol^{-1}$	K	$J \cdot K^{-1} \cdot mol^{-1}$	K	$J \cdot K^{-1} \cdot mol^{-1}$
Series 1		156.80	21.48	274.14	24.67
56.19	9.633	158.66	21.57	276.28	24.71
57.63	9.960	160.50	21.68	278.42	24.77
59.13	10.30	162.34	21.75	280.55	24.78
60.72	10.65	164.23	21.83	282.68	24.85
62.39	11.01	166.17	21.93	284.80	24.87
64.10	11.38	168.13	22.01	286.92	24.87
65.77	11.72	170.11	22.09	289.04	24.93
67.38	12.05	172.09	22.17	291.15	24.95
68.94	12.36	174.10	22.24	293.25	24.99
70.45	12.65	176.09	22.32	295.36	25.00
71.96	12.93	178.07	22.40	297.45	25.05
73.48	13.21	180.05	22.47	299.55	25.12
75.06	13.50	182.01	22.54	301.64	25.12
76.57	13.76	183.97	22.62	Series 3	
78.07	14.02	185.92	22.69	12.62	0.3979
79.64	14.28	187.87	22.76	13.60	0.4759
81.21	14.53	189.80	22.82	14.79	0.6000
82.79	14.78	191.80	22.87	16.00	0.7378
84.41	15.03	193.84	22.95	17.19	0.8831
86.05	15.27	195.89	23.03	18.37	1.038
87.72	15.53	197.92	23.09	19.55	1.206
89.44	15.77	199.95	23.15	20.77	1.394
91.18	16.01	202.02	23.20	22.04	1.606
92.93	16.24	204.14	23.27	23.39	1.846
94.69	16.47	206.24	23.33	24.77	2.111
96.46	16.69	208.34	23.39	26.20	2.396
98.25	16.92	210.44	23.44	27.65	2.699
100.05	17.13	212.53	23.47	29.02	2.994
101.86	17.34	214.61	23.53	30.39	3.306
103.69	17.54	216.68	23.60	31.86	3.644
105.58	17.74	218.75	23.64	33.38	4.002
107.50	17.95	220.81	23.75	34.92	4.375
109.40	18.14	222.87	23.75	36.45	4.751
111.27	18.32	224.92	23.79	37.97	5.127
113.15	18.50	226.97	23.85	39.49	5.512
115.02	18.67	229.01	23.89	41.04	5.901
116.87	18.85	231.07	23.92	42.64	6.304
118.70	19.00	233.15	24.00	44.26	6.718
122.30	19.30	235.22	24.04	45.88	7.125
124.08	19.44	237.29	24.08	47.49	7.528
125.91	19.60	239.36	24.12	49.10	7.927
Series 2		241.42	24.12	50.67	8.313
127.81	19.73	243.47	24.18	52.23	8.692
129.75	19.87	245.52	24.21	53.92	9.095
131.75	20.01	247.56	24.25	55.64	9.499
133.73	20.15	249.60	24.29	57.33	9.886
135.69	20.27	251.63	24.33	59.00	10.27
137.64	20.41	253.66	24.39	60.65	10.63
139.60	20.54	255.68	24.43	62.23	10.98
141.56	20.65	257.70	24.45	63.87	11.32
143.51	20.77	259.71	24.48	65.55	11.67
145.45	20.88	261.72	24.49	67.18	12.00
147.37	20.99	263.73	24.54	68.77	12.32
149.28	21.09	265.75	24.56	70.30	12.62
151.18	21.20	267.80	24.60	71.80	12.90
153.06	21.30	269.87	24.67	73.26	13.17
154.94	21.39	271.99	24.67	74.69	13.43

samples (samples a, b, and c). However, the heat capacity of the crystallized sample (sample d) is larger than that of sample c between (40 and 110) K, while it is the smallest below 40 K and above 110 K.

It is well-known that the heat capacity includes various contributions, i.e., lattice vibrations, electronic contributions, energy levels formed by crystal-field splitting in magnetic materials, etc. In addition, the heat capacity of glassy materials includes the characteristic boson peak at several tens of kelvin and the T -linear term at very low temperatures caused by disorder nature in the glassy state. In the lowest

Table 2. Measured Molar Heat Capacity of the Crystallized (in a Vacuum at 877 K) Ribbon Sample of $Zr_{0.55}Al_{0.10}Ni_{0.05}Cu_{0.30}$

T	C_p	T	C_p	T	C_p
K	$J \cdot K^{-1} \cdot mol^{-1}$	K	$J \cdot K^{-1} \cdot mol^{-1}$	K	$J \cdot K^{-1} \cdot mol^{-1}$
Series 1		89.45	15.64	188.27	22.51
13.47	0.3320	90.81	15.83	190.29	22.57
14.55	0.4274	92.19	16.01	192.32	22.63
15.64	0.5388	93.60	16.20	194.34	22.69
16.77	0.6588	95.06	16.38	196.37	22.75
17.94	0.7962	96.56	16.57	198.42	22.81
19.13	0.9493	98.12	16.76	200.49	22.87
20.33	1.118	99.73	16.95	202.54	22.91
21.54	1.306	101.42	17.14	204.59	22.98
22.76	1.512	103.17	17.33	206.64	23.05
24.06	1.748	104.94	17.52	208.68	23.08
25.42	2.013	106.72	17.71	210.71	23.13
26.75	2.281	108.48	17.89	212.73	23.16
28.08	2.562	110.25	18.06	214.75	23.22
29.43	2.860	112.01	18.23	216.77	23.26
30.82	3.176	113.76	18.40	218.78	23.32
32.23	3.507	115.51	18.56	220.79	23.37
33.59	3.833	117.27	18.72	222.82	23.47
34.92	4.156	119.04	18.86	224.84	23.47
36.23	4.489	120.82	19.01	226.86	23.50
37.57	4.822	122.59	19.14	228.87	23.56
38.92	5.169	124.36	19.29	230.87	23.58
40.27	5.510	126.14	19.44	232.89	23.64
41.64	5.865	Series 2		234.91	23.69
43.02	6.219	127.93	19.57	236.93	23.74
44.43	6.582	129.71	19.71	238.95	23.77
45.85	6.944	131.50	19.83	240.92	23.80
47.23	7.294	133.30	19.93	242.86	23.83
48.60	7.640	135.11	20.04	244.77	23.86
50.02	7.993	136.95	20.18	246.65	23.89
51.43	8.347	138.80	20.29	248.54	23.93
52.86	8.692	140.64	20.41	250.44	23.95
54.30	9.038	142.47	20.50	252.33	24.00
55.71	9.371	144.28	20.61	254.22	24.05
57.10	9.695	146.09	20.72	256.12	24.08
58.51	10.02	147.89	20.82	258.09	24.11
59.94	10.34	149.68	20.92	260.07	24.14
61.37	10.66	151.46	21.00	262.05	24.13
62.81	10.97	153.23	21.09	264.06	24.17
64.28	11.28	154.99	21.18	266.09	24.21
65.76	11.59	156.78	21.25	268.15	24.22
67.23	11.89	158.63	21.36	270.24	24.27
68.73	12.19	160.53	21.45	272.33	24.33
70.23	12.48	162.40	21.55	274.41	24.28
71.72	12.76	164.29	21.61	276.49	24.31
73.22	13.04	166.22	21.69	278.56	24.36
74.73	13.31	168.16	21.78	280.63	24.39
76.24	13.58	170.11	21.86	282.70	24.45
77.75	13.84	172.10	21.94	284.76	24.48
79.25	14.09	174.13	22.00	286.82	24.47
80.75	14.33	176.15	22.08	288.88	24.51
82.29	14.58	178.18	22.15	290.94	24.55
83.84	14.82	180.19	22.23	293.02	24.57
85.30	15.04	182.21	22.28	295.10	24.55
86.71	15.25	184.24	22.37	297.17	24.57
88.09	15.45	186.25	22.43	299.24	24.60

temperature region from 13 K to 40 K, in general, a material of small heat capacity should be harder than that of a material of large heat capacity, and have higher sound velocity and higher elastic constant. The density and sound velocity of glassy ZNC increase by annealing and then by crystallization.⁶ The present results of the heat capacity measurements show a good agreement with those elastic properties. The hump in the curve of ΔC_p around 25 K may be a boson peak, which is commonly observed in glassy materials.

In the temperature range from 40 K to 110 K, the heat capacity of the crystallized sample (sample d) is larger than that of sample c but smaller than those of the other glassy samples (samples a and b). In this temperature range, the

Table 3. Thermodynamic Functions of the As-Prepared Ribbon Sample of $Zr_{0.55}Al_{0.10}Ni_{0.05}Cu_{0.30}$ ^a

T	$C_{p,m}^{\circ}$	$\Delta_0^{\circ}H_m^{\circ}$	$\Delta_0^{\circ}S_m^{\circ}$
K	$J \cdot K^{-1} \cdot mol^{-1}$	$J \cdot mol^{-1}$	$J \cdot K^{-1} \cdot mol^{-1}$
15	0.624	2.701	0.2727
20	1.274	7.357	0.5362
30	3.216	29.21	1.396
40	5.639	73.26	2.646
50	8.149	142.3	4.175
60	10.49	235.7	5.872
70	12.56	351.2	7.648
80	14.34	485.9	9.445
90	15.85	637.0	11.22
100	17.12	802.0	12.96
110	18.20	978.8	14.64
120	19.12	1165	16.27
130	19.89	1361	17.83
140	20.56	1563	19.33
150	21.14	1771	20.77
160	21.64	1985	22.15
170	22.08	2204	23.47
180	22.47	2427	24.75
190	22.83	2653	25.97
200	23.15	2883	27.15
210	23.43	3116	28.29
220	23.68	3352	29.38
230	23.91	3590	30.44
240	24.12	3830	31.46
250	24.31	4072	32.45
260	24.48	4316	33.41
270	24.64	4562	34.33
280	24.78	4809	35.23
290	24.94	5057	36.10
298.15	25.07	5261	36.80
300	25.10	5307	36.95

^a $C_{p,m}^{\circ}$: standard molar heat capacity. $\Delta_0^{\circ}H_m^{\circ}$: the standard molar enthalpy. $\Delta_0^{\circ}S_m^{\circ}$: standard molar entropy.

nonacoustic and/or local lattice vibrations become thermally excited, and the present results show that the local structure of the crystallized sample is much different from that of sample c. As the crystallized sample includes several crystalline phases, such as Zr_2Cu , Zr_2Ni , etc.,^{1,3,4,17} it may have a different local structure from that of the glassy state. Above 110 K, the electronic contribution (T -linear term) becomes dominant.

To see the effect of annealing in the glassy state, the difference between the heat capacity of the glassy samples ($\Delta C_p = C_{p(a,b)} - C_{p(c)}$) is plotted in Figure 4. The heat capacity difference can be fitted to

$$\Delta C = C_{Sch} + \gamma T$$

The C_{Sch} denotes Schottky-type heat capacity of a two level system that can be given by a difference in two Einstein-type heat capacities (C_{Ein}) with frequencies ν and 2ν as follows:

$$C_{Sch}(h\nu, T) = C_{Ein}(h\nu, T) - C_{Ein}(2h\nu, T)$$

where h is Planck's constant. The right-hand side of the equation means the softening of the phonon mode that is the change of the vibration frequency from $2h\nu$ to $h\nu$. It is well-known that the maximum temperature T_{max} in the Schottky-type heat capacity curve is represented as $k_B T_{max}/h\nu = 0.42$. Thus, the frequency ν is estimated to be about 2 THz. This indicates that the excess heat capacity is attributed to the softening of the lattice vibrations in the as-prepared ribbon glassy sample (sample a). The present results show that the frequencies of lattice vibrations become higher by the annealing. Above 100 K, the T -linear term γT is dominant in $\Delta C_p (= C_{p(a,b)} - C_{p(c)})$. It should be related to the difference in the contribution of the

Table 4. Thermodynamic Functions of the Crystallized (at 877 K in a Vacuum) Ribbon Sample of $Zr_{0.55}Al_{0.10}Ni_{0.05}Cu_{0.30}$ ^a

T	$C_{p,m}^{\circ}$	$\Delta_0^{\circ}H_m^{\circ}$	$\Delta_0^{\circ}S_m^{\circ}$	Φ_m°
K	$J \cdot K^{-1} \cdot mol^{-1}$	$J \cdot mol^{-1}$	$J \cdot K^{-1} \cdot mol^{-1}$	$J \cdot K^{-1} \cdot mol^{-1}$
15	0.471	1.801	0.1641	0.0441
20	1.070	5.565	0.3766	0.0984
30	2.988	25.18	1.146	0.3064
40	5.443	67.09	2.334	0.6571
50	7.990	134.3	3.824	1.138
60	10.357	226.3	5.494	1.723
70	12.44	340.5	7.250	2.386
80	14.21	474.0	9.030	3.106
90	15.72	623.8	10.79	3.862
100	16.97	787.5	12.52	4.642
110	18.04	962.7	14.19	5.434
120	18.94	1148	15.80	6.231
130	19.72	1341	17.34	7.026
140	20.36	1542	18.83	7.817
150	20.93	1748	20.25	8.599
160	21.42	1960	21.62	9.370
170	21.85	2176	22.93	10.13
180	22.22	2397	24.19	10.88
190	22.56	2621	25.40	11.61
200	22.86	2848	26.57	12.33
210	23.11	3078	27.69	13.03
220	23.34	3310	28.77	13.72
230	23.58	3544	29.81	14.40
240	23.78	3781	30.82	15.06
250	23.95	4020	31.79	15.71
260	24.12	4260	32.74	16.35
270	24.26	4502	33.65	16.97
280	24.40	4746	34.53	17.59
290	24.51	4990	35.39	18.18
298.15	24.59	5190	36.07	18.66
300	24.61	5236	36.22	18.77

^a $C_{p,m}^{\circ}$: standard molar heat capacity. $\Delta_0^{\circ}H_m^{\circ}$: the standard molar enthalpy. $\Delta_0^{\circ}S_m^{\circ}$: the standard molar entropy. $\Phi_m^{\circ} = \Delta_0^{\circ}S_m^{\circ} - \Delta_0^{\circ}H_m^{\circ}/T$.

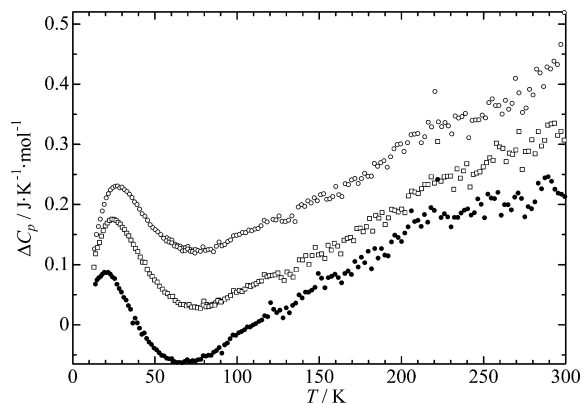


Figure 3. Heat capacity difference $\Delta C_p = C_{p(a,b,c)} - C_{p(d)}$ between the glassy samples (samples a–c) and the crystallized sample (sample d) of ZANC: \circ , as-prepared glassy (a); \square , annealed at 508 K in a vacuum (b); \bullet , annealed at 641 K in a vacuum (c).

conduction electron, and may indicate that the density of state of the electrons at the Fermi energy level in the glass samples decreases by annealing.

Conclusions

The precise heat capacity of the $Zr_{0.55}Al_{0.10}Ni_{0.05}Cu_{0.30}$ alloy was measured for the as-prepared glassy, annealed, and crystallized ribbon samples by adiabatic calorimetry from 13 K to 300 K, and the values of standard enthalpy, entropy, and Gibbs energy were calculated for the as-prepared glassy and the crystallized ZANC. The heat capacity difference among the as-prepared glassy, annealed, and crystallized

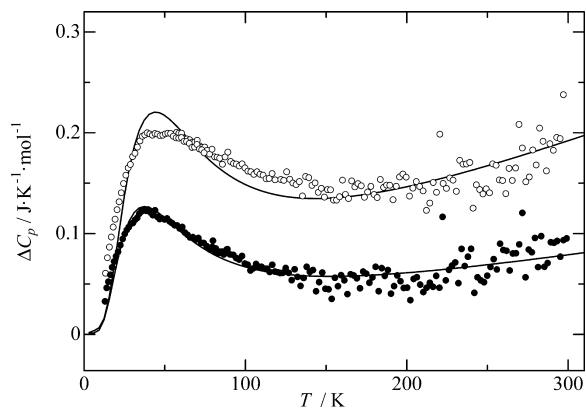


Figure 4. Heat capacity difference ΔC_p of the glassy samples (samples a and b) from the glassy sample annealed at 641 K (sample c) of ZANC: ○, $\Delta C_p = C_{p(a)} - C_{p(c)}$; ●, $\Delta C_p = C_{p(b)} - C_{p(c)}$. Solid lines denote the fitted curve of Schottky type heat capacity.

samples were analyzed and discussed, which coincided with those of ultrasonic and hardness, and density measurements of ZANC.^{6,8} The heat capacity difference among the glassy ribbon, glassy rod and their crystallized samples will be discussed further in detail.¹⁸

Literature Cited

- (1) Shoji, T.; Inoue, A. Hydrogen absorption and desorption behavior of Zr-Based amorphous alloys with a large structurally relaxed amorphous region. *J. Alloys Comp.* **1999**, *292*, 275–280.
- (2) Zhang, T.; Inoue, A.; Masumoto, T. Amorphous Zr-Al-TM(TM = Co, Ni, Cu) Alloys with Significant Supercooled Liquid Region of Over 100 K. *Mater. Trans., JIM* **1991**, *32*, 1005–1010.
- (3) Inoue, A. Stabilization of Metallic Supercooled Liquid and Bulk Amorphous Alloys. *Acta Mater.* **2000**, *48*, 279–306.
- (4) Inoue, A.; Negishi, T.; Kimura, H. M.; Zhang, T.; Yavari, A. R. High Packing Density of Zr- and Pd-Based Bulk Amorphous Alloys. *Mater. Trans., JIM* **1998**, *39*, 318–321.
- (5) Inoue, A.; Masumoto, T.; Chen, H. S. Enthalpy Relaxation Behaviour of (Fe, Co, Ni)₇₅Si₁₀B₁₅ Amorphous Alloys upon Low Temperature Annealing. *J. Mater. Sci.* **1984**, *19*, 3953–3966.

- (6) Tamura, S.; Fukuhara, M.; Inoue, A. Changes in Mechanical Properties of Zr-Based Bulk Metallic Glass under Linear Heating and Cooling. *J. Appl. Phys.* **2007**, *101*, 073520–1073520–6.
- (7) Maeda, M.; Takahashi, Y.; Fukuhara, M.; Wang, X.; Inoue, A. Ultrasonic Bonding of Zr₅₅Cu₃₀Ni₅Al₁₀ Metallic Glass. *Mater. Sci. Eng., B* **2008**, *148*, 141–144.
- (8) Slipenyuk, A.; Eckert, J. Correlation between Enthalpy Change and Free Volume Reduction during Structural Relaxation of Zr₅₅Cu₃₀Ni₅Al₁₀ Metallic Glass. *Scripta Mater.* **2004**, *50*, 39–44.
- (9) Moriya, Y.; Yoshida, T.; Kawaji, H.; Atake, T.; Fukuhara, M.; Kimura, H.; Inoue, A. Heat Capacity of Glassy and Crystalline Zr_{0.55}-Al_{0.10}Ni_{0.05}Cu_{0.30}. *Mater. Sci. Eng., B* **2008**, *148*, 207–210.
- (10) Fukuhara, M.; Wang, X.; Inoue, A. Thermal Elasticity in Glassy Alloys based on Topology of Metallic Clusters. *Appl. Phys. Lett.* **2007**, *91*, 171908–171908–3.
- (11) Moriya, Y.; Yoshida, T.; Kawaji, H.; Atake, T.; Fukuhara, M.; Kimura, H.; Inoue, A. In *Glass Transition Phenomena and Heat Capacity of High Quality Advanced Materials II: Ceram. Trans.*; Ewsuk, K., Ed.; John Wiley & Sons, Inc.: Hoboken, NJ 2007; Vol. 198, pp 117–122.
- (12) Moriya, Y.; Yoshida, T.; Kawaji, H.; Atake, T.; Fukuhara, M.; Kimura, H.; Inoue, A. Heat Capacity Measurements on a Thin Ribbon Sample of Zr_{0.55}Al_{0.10}Ni_{0.05}Cu_{0.30} Glassy Alloy and Apiezone N High Vacuum Grease Using a Quantum Design Physical Property Measurement System. *Cryogenics* **2009**, *49*, 185–191.
- (13) Yamaura, S.; Sakurai, M.; Hasegawa, M.; Wakoh, K.; Shimpō, Y.; Nishida, M.; Kimura, H.; Matsubara, E.; Inoue, A. Hydrogen Permeation and Structural Features of Melt-spun Ni-Nb-Zr Amorphous Alloys. *Mater.* **2005**, *53*, 3703–3711.
- (14) Uchida, A.; Moriya, Y.; Kawaji, H.; Atake, T.; Fukuhara, M.; Kimura, H.; Inoue, A. To be published.
- (15) Atake, T.; Kawaji, H.; Hamano, A.; Saito, Y. Construction of an Adiabatic Calorimeter for Heat Capacity Measurement from Liquid Helium Temperature to 330 K. *Rep. Res. Lab. Eng. Mater., Tokyo Inst. Technol.* **1990**, *15*, 13–23.
- (16) Tanaka, T.; Atake, T.; Nakayama, H.; Eguchi, T.; Saito, K.; Ikemoto, I. Heat Capacity and incommensurate phase transition of crystalline bis (4-chlorophenyl) Sulfone. *J. Chem. Thermodyn.* **1994**, *26*, 1231–1239.
- (17) Fan, C.; Takeuchi, A.; Inoue, A. Preparation and Mechanical Properties of Zr-Based Bulk Nanocrystalline Alloys Containing Compound and Amorphous Phases. *Mater. Trans., JIM* **1999**, *40*, 42–51.
- (18) Uchida, A.; Moriya, Y.; Kawaji, H.; Atake, T.; Fukuhara, M.; Kimura, H.; Inoue, A. To be published.

Received for review November 17, 2008. Accepted April 4, 2009.

JE8008733